Electrochemical Behavior of $Ti_3C_2T_x$ MXene in Environmentally Friendly Methanesulfonic Acid Electrolyte

Xin Zhao[a], Chunxiang Dall'Agnese[a], Xue-Feng Chu[b], Shuangshuang Zhao[a], Gang Chen[a,c], Yury Gogotsi[a,d], Yu Gao[a,*], Yohan Dall'Agnese[e,*]

Abstract: Two-dimensional transition metal carbides, nitrides and carbonitrides called MXenes have gained much attention as electrode materials in electrochemical energy storage devices. In particular, $Ti_3C_2T_x$ achieved outstanding performance in common sulfuric acid (H_2SO_4) electrolyte. In this work, a more environmentally friendly alternative acidic electrolyte, methanesulfonic acid (MSA CH_3SO_3H) is proposed. The energy storage performance of $Ti_3C_2T_x$ in aqueous and neat MSA ionic liquid electrolytes is investigated. The specific capacitance of 298 F g^{-1} was obtained at a scan rate of 5 mVs^{-1} in 4 M MSA and it exhibits excellent cycle stability with retention of nearly 100% over 10,000 cycles. This electrochemical performance is similar to that of $Ti_3C_2T_x$ in H_2SO_4, but using a greener electrolyte. *In-situ* X-ray diffraction analysis reveals the intercalation charge storage mechanism. Specifically, the lattice changes up to 5.16 Å during cycling, which is the largest reversible volume change observed in MXenes in aqueous electrolytes.

Introduction

Two-dimensional (2D) materials, most notably graphene, have attracted considerable interest because of their optoelectronic and chemical properties. One of the larger families of 2D materials is the transition metal carbides, carbonitrides and nitrides called MXenes, of general formula $M_{n+1}X_nT_x$, where M represents early transition metals (i.e, Sc, Ti, V, Cr, Zr, Hf, Nb, Mo, Ta, and W), X is carbon and/or nitrogen, T_x stands for the surface terminations (hydroxyl, oxygen or fluorine), and n=1, 2 or 3.[1] MXenes are usually synthesized by chemical etching and exfoliation of ternary ceramics of general formula $M_{n+1}AX_n$, with A standing for Al, Si, or Ga.[1a, 2] So far, more than thirty different chemical compositions of MXenes have been experimentally obtained, and many more have been theoretically predicted. MXenes, in particular $Ti_3C_2T_x$, the first discovered and most investigated MXene, have been studied for energy storage,[3] sensors,[4] adsorption materials,[5] catalysis,[6] electromagnetic interference shielding,[7] solar cells,[8] medical applications,[9] and so on.

Improving supercapacitors is one of the key energy storage challenges as they are complementary to batteries and important in renewable energy production as well as many other technologies. MXenes are remarkable electrode materials for supercapacitors, because of their metallic conductivity and hydrophilic tuneable transition metal oxide-like surface termination that can undergo redox reactions, which highlight them as competitive alternatives to other electrode materials.[1a, 3b] Several MXenes, including $Ti_3C_2T_x$,[10] Ti_2CT_x,[11] Mo_2CT_x,[12] $Mo_{1.33}CT_x$,[13] and V_2CT_x,[14] have emerged as promising electrodes for supercapacitors. The first and most investigated one for this application is $Ti_3C_2T_x$ which exhibits outstanding performance. The electrochemical behavior of $Ti_3C_2T_x$ in a wide variety of electrolytes, including various aqueous, organic, and ionic liquid electrolytes has been reported.[15] The best electrochemical performance is obtained in sulfuric acid (H_2SO_4), notably, capacitance up to 450 F g^{-1} and 1,500 F cm^{-3} was achieved using thin electrode (90 nm thick) and a hydrogel respectively.[16] The electrochemical reaction in acidic electrolyte was proposed to follow equation:

$$Ti_3C_2O_x(OH)_yF_z + \delta H^+ + \delta e^- \leftrightarrow Ti_3C_2O_{x-\delta}(OH)_{y+\delta}F_z \qquad (1)$$
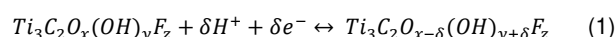
However, H_2SO_4 for wearable devices and other applications, where safety is major issue, safer and greener electrolytes should be explored. So far, electrochemical performance in other electrolytes has been significantly lower, including neutral sulfate electrolytes such as Li_2SO_4 or Na_2SO_4.[17] It can be deduced that the excellent capacitance in H_2SO_4 is mostly attributed to proton intercalation and adsorption.

Research on MXenes' behavior in other acidic electrolytes should lead to further insights in the fundamental mechanism of charge storage as well as improved potential for practical application. Methanesulfonic acid (MSA, CH_3SO_3H) is considered a natural product with a low toxicity. It is also readily biodegradable, ultimately forming sulfates and carbon dioxide. Aqueous solution of MSA does not involve any dangerous volatile chemicals under normal conditions. Besides, MSA has excellent metal salts solubility, exceeding in sulfuric acid.[18] The conductivity of MSA is comparable to other strong acids such as H_2SO_4 and hydrochloric

[a]   X. Zhao, Dr. C. Dall'Agnese, S. S. Zhao, Prof. G. Chen, Prof. Y.
         Gogotsi, Prof. Y. Gao
         Kay Laboratory of Physics and Technology for Advanced Batteries
         (Ministry of Education), College of Physics
         Jilin University
         Changchun, 130012 (P.R. China)
         E-mail: yugao@jlu.edu.cn
[b]   Dr. X. Chu
         Key Laboratory of Architectural Cold Climate Energy Management
         Jilin Jianzhu University,
         Changchun, 130118 (P.R. China)
[c]   Prof. G. Chen
         State Key Laboratory of Superhard Materials, College of Physics
         Jilin University
         Changchun, 130012 (P.R. China)
[d]   Prof. Y. Gogotsi
          A. J. Drexel Nanomaterials Institute Department of Materials
          Science and Engineering
         Drexel University
         Philadelphia, PA 19104 (USA)
[e]   Dr. Y. Dall'Agnese
         Institute for Materials Discovery
         University College London
         Roberts Building, Room 107, Malet Place
         London WC1E 7JE (United Kingdom)
         E-mail: y.dallagnese@ucl.ac.uk

FULL PAPER

acid.[19] MSA has been used in industry for more than 20 years, mostly because of its excellent properties for electroplating tin. MSA is also among the most suitable electrolytes in redox flow batteries.[20] Therefore, in this article, the electrochemical behavior of $Ti_3C_2T_x$ in aqueous and neat ionic liquid MSA are investigated. We demonstrate that MSA is a promising greener alternative electrolyte for supercapacitors. Indeed, the electrochemical performance of $Ti_3C_2T_x$ in 4 M MSA is about as good as in H_2SO_4. Additionally, the charge storage mechanism is investigated via *in-situ* X-ray diffraction (XRD) and a 4.6 Å large expansion and shrinkage phenomenon is revealed.

Results and Discussion

Figures 1a-d show the cyclic voltammograms of $Ti_3C_2T_x$ tested in different concentrations of MSA, from 1 M aqueous solution to neat ionic liquid. The stability windows are larger than 1 V which is suitable for aqueous supercapacitor materials. In all electrolytes, the cyclic voltammograms present redox peaks, unlike conventional carbon-based supercapacitor materials with rectangular cyclic voltammograms. However, this is not surprising as it was previously reported that MXenes can undergo redox reactions and exhibit pseudocapacitive behaviors.[10, 21] In regard to the working potential ranges, the redox peaks potentials, and the capacitance, it appears that the electrochemical behavior of
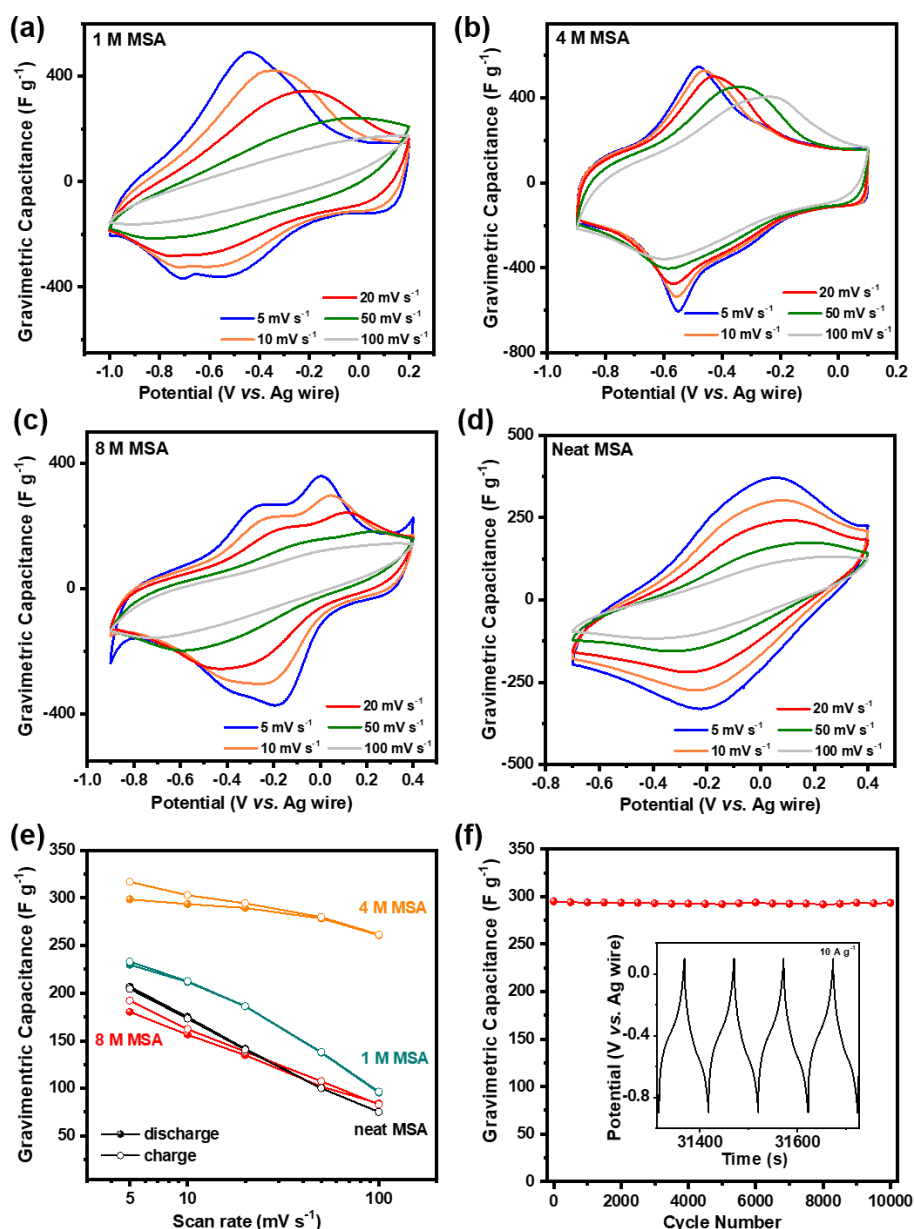

Figure 1. Cyclic voltammograms of $Ti_3C_2T_x$ in (a) 1 M, (b) 4 M, (c) 8 M, and (d) neat MSA electrolytes at different scan rates. (e) Summary of the capacitance with the potential scan rate. (f) Cycle life of $Ti_3C_2T_x$ in 4 M MSA measured from galvanostatic charge - discharge at 10 A g^{-1} and the corresponding charge-discharge profile (inset).

$Ti_3C_2T_x$ is significantly different at each concentration. In 1 M, 4 M,

and 8 M aqueous MSA electrolytes, two redox reaction couples can be distinguished, whereas only one redox couple with broader peaks can be identified in neat MSA. Although the corresponding peak potentials and intensities are different at each concentration, they are probably due to the same electrochemical phenomena. (intercalation and adsorption of protons). The difference might come from an effect of the solvation shell, similarly to the one recently observed for $Ti_3C_2T_x$ in LiTFSI.[22] Interestingly, $Ti_3C_2T_x$ in 4 M MSA presents the sharpest redox peaks among all electrolytes tested so far, resulting in an electrochemical behavior closer to batteries than electrochemical double layer capacitors (*i.e,* the conventional type of supercapacitors).

Figure 1e summarizes the specific capacitances obtained in each concentration of MSA at different scan rates. The best performances, up to 298 F g^{-1}, are achieved in 4 M MSA, possibly due to synergetic effect between conductivity and solvation. The performances at high rates show reasonable capacitance retention, for example, 87% retention in the case of 4 M MSA at 100 mV s^{-1}, which is suitable for high power applications. The performance dependence on scan rate is correlated to kinetics and ohmic limitations observed by the increasing distance between redox peaks in CV curves. This is attributed to the fact that horizontally restacked nanosheets impede high ion diffusivity through the electrode. It is worth mentioning that although it was previously reported that rate performance of MXene electrodes can be greatly improved if open architecture are used, such as macroporous structure,[16] vertically aligned nanosheets,[23] or composites with spacers between layers,[24] it is not the goal of this work.

For practical application, commercial supercapacitors need to have excellent capacitance retention. To further investigate the suitability of $Ti_3C_2T_x$ in 4 M MSA for supercapacitors, the cycle life was tested by galvanostatic charge-discharge at a high current density of 10 A g^{-1}, as shown Figure 1f. Excellent capacitance retention was observed, as a specific capacitance of 293 F g^{-1} was maintained after 10,000 cycles.

In-situ XRD analysis of $Ti_3C_2T_x$ in 4 M MSA was performed to understand the charge storage mechanism. Figure 2a shows the *in-situ* XRD patterns during cyclic voltammetry at 0.2 mV s^{-1} with the XRD peak corresponding to the (002) peak of $Ti_3C_2T_x$. It is worth noting that after immersion in electrolyte and first few cycles, intercalation of water molecules and solvated ions between $Ti_3C_2T_x$ layers occured,[25] which explained the shift from the dry electrode, but was not further investigated here. Using Bragg's equation, Figure 2b represents the calculated *c*-lattice parameters, which are directly proportional to the interlayer distances between $Ti_3C_2T_x$ layers. *In-situ* XRD analysis reveals that abrupt lattice spacing changes occur from -0.5 V to -0.4 V during reduction and from -0.4 V to -0.3 V during oxidation, that is to say at potentials around the sharp redox couple on CV curves (Fig.1). Outside of the region of these redox peaks, only slight changes of the *c*-
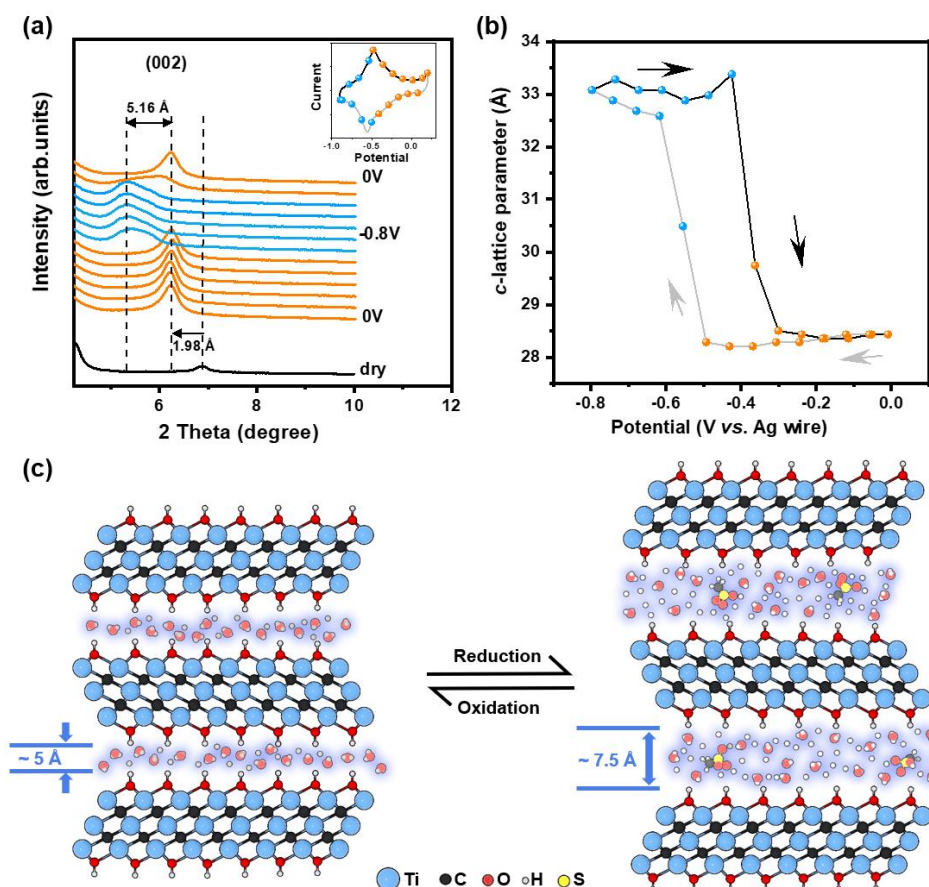

Figure 2. *In-situ* X-ray diffraction analysis of $Ti_3C_2T_x$ in 4 M MSA: (a) XRD patterns during cycling and (b) corresponding *c*-lattice parameter vs. Potential, and (c) schematic of a charge storage mechanism hypotheses.

lattice parameter are recorded. Overall, during an electrochemical cycle, the c-lattice parameter reversibly expanded and shrunk by up to 5.16 Å, corresponding to a 2.58 Å change in $Ti_3C_2T_x$ interlayer distance. This is the largest volume change reported for MXenes in aqueous electrolytes and larger than the case of H_2SO_4.[25a]

As the sharp redox peaks are at potential lower than the open circuit voltage (OCV = -0.03V $vs.$ Ag), it can be proposed that the electrochemical mechanism is attributed to cation intercalation and adsorption, which is H^+ or H_3O^+ in 4 M MSA. But in either case, the recorded volume change is too large to be attributed to a single layer of cation intercalation. This induce that the mechanism is either the intercalation of cation with large solvation
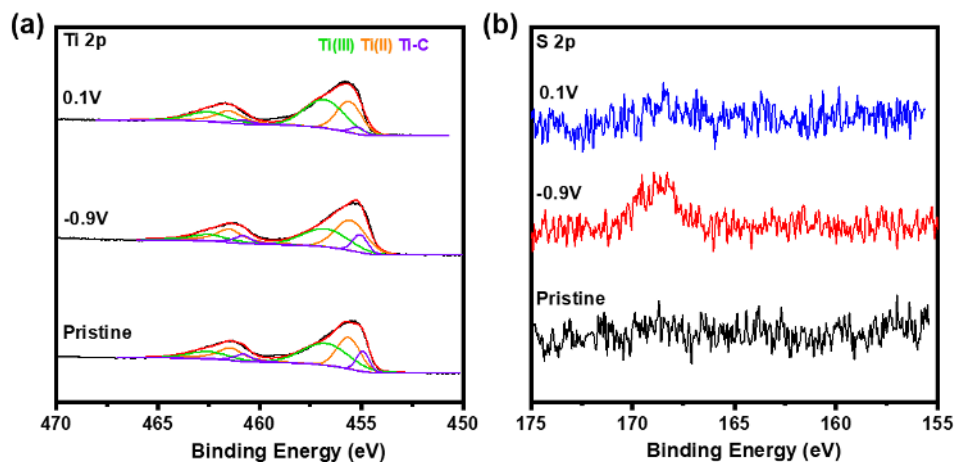

Figure 3. High-resolution XPS spectra in (a) the Ti 2p and (b) S2p regions of pristine $Ti_3C_2T_x$, and $Ti_3C_2T_x$ after cycling and polarization at -0.9 V and 0.1 V $vs.$ Ag.
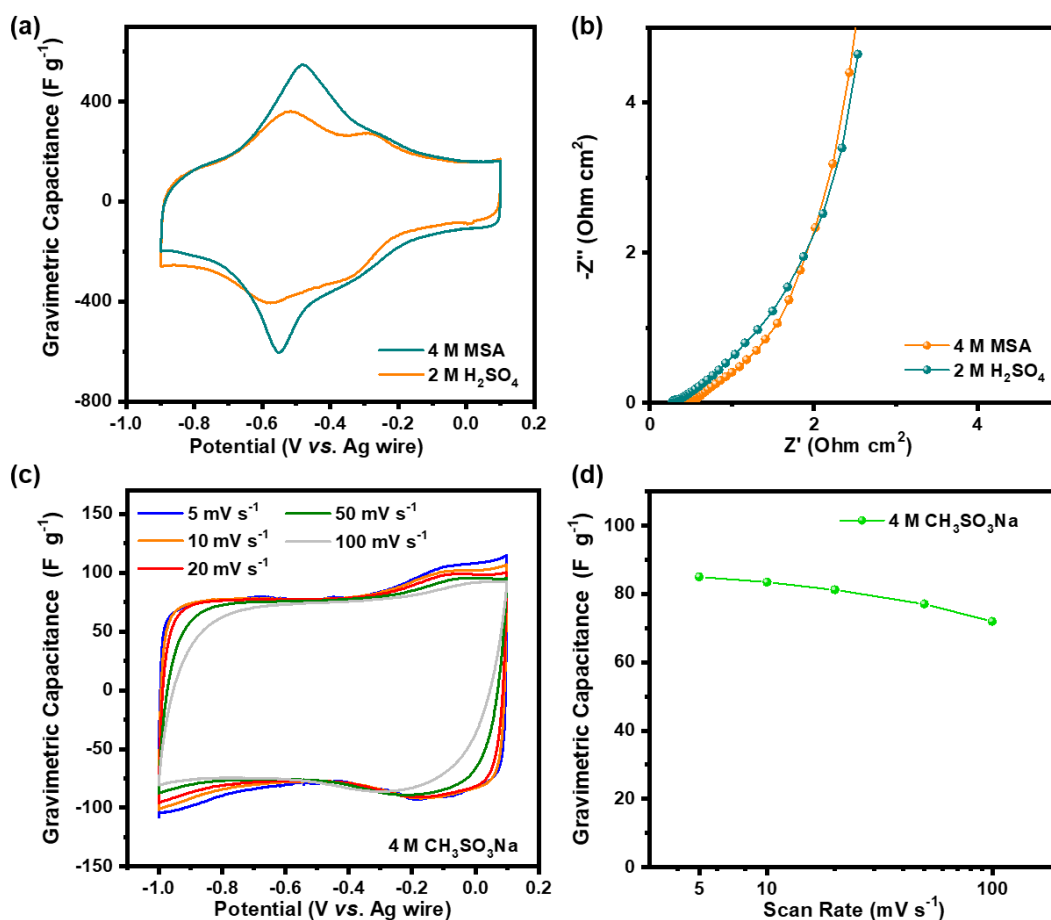

Figure 4. Comparison of electrochemical behavior of $Ti_3C_2T_x$ in 2 M H_2SO_4 and 4 M MSA: (a) cyclic voltammograms at 5 mV s^{-1} and (b) Nyquist plot, (c) cyclic voltammograms and (d) rate performance of $Ti_3C_2T_x$ in 4 M CH_3SO_3Na.

shell, or the formation of several layers of cations between $Ti_3C_2T_x$ layers, or the co-intercalation of $CH_3SO_3^-$ anions, or a combination of these. The latter hypothesis, represented in Figure 2c, is highly probable because of the following reasons: (i) cation and organic molecules intercalation were previously reported,[10, 26] (ii) MSA has a size around 2.5 Å and is an ionic liquid, which are known to be difficult to dissociate and tend to co-intercalate,[27] (iii) in the CH_3SO_3H--H_2O system, $CH_3SO_3^-$ might be in a complex with a molecule of the acid, in contrast to aqueous solutions of H_2SO_4,[28] and (iv) it was reported that several layers of H_2O can be intercalated between MXene layers.[25b]

To identify the surface chemistry and intercalated species, XPS measurements were performed on pristine $Ti_3C_2T_x$ and electrodes polarized for 2 hours at -0.9 V and 0.1 V vs. Ag in 4 M MSA. High-resolution XPS spectra in Ti 2p, C 1s and S 2p regions are shown in Figure 3. The Ti 2p spectrum can be deconvoluted into three peaks corresponding to Ti (II) (455.8 eV), Ti (III) (457.1 eV) and C–Ti (460.2 eV), and this is consistent with the literature.[29] As expected, high-resolution XPS spectra in the S 2p region indicate that the pristine $Ti_3C_2T_x$ sample does not contain sulfur. However, after polarization at -0.9 V vs. Ag, S is detected on the surface, suggesting adsorption or intercalation of $CH_3SO_3^-$. To attempt to identify the charge storage mechanism of $Ti_3C_2T_x$ in 4 M MSA, the electrochemical behavior with closely related electrolytes was recorded. 2 M H_2SO_4 and 4 M CH_3SO_3Na were selected because the former has the same cation and is the standard acidic electrolyte, and the latter has the same anion. Figures 4a-b compare the cyclic voltammograms and Nyquist plots in 4 M MSA and 2 M H_2SO_4. The capacitance in 2 M H_2SO_4 was 254 F g^{-1} which is somewhat lower than the best performance of $Ti_3C_2T_x$ reported in sulfuric acid, but it can be attributed to thicker restacked electrodes. Two pairs of redox peaks are observed at the same potentials in both CV curves; thus, these peaks could be attributed to proton intercalation and adsorption from Equation 1. The difference in intensity could be due to solvation shell, anion co-intercalation, or electrolyte resistance. EIS results further demonstrate similarities in the behavior of these two electrolytes and correspond to typical supercapacitor materials. Besides, because the x-axis intercepts in these Nyquist plots correspond to electrolyte resistance, it can be noted that the ionic conductivity of 2 M H_2SO_4 is slightly superior to 4 M MSA. One would expect the sharpest redox peaks to be in the most conductive electrolyte, but it is not the case here.

Figures 4c-d show that electrochemical behavior of $Ti_3C_2T_x$ in 4 M CH_3SO_3Na is totally different than in 4 M MSA. The energy storage performance in CH_3SO_3Na is significantly inferior, with the highest capacitance up to 95 F g^{-1}. The cyclic voltammograms do not exhibits sharp redox peaks and are quasi-rectangular, suggesting primarily the double-layer energy storage mechanism. This further implies that the sharp redox peaks observed in 4 M MSA were due to proton reactions and not from anion. However, further complementary experiments are needed to fully identify the interlayer composition.

Conclusions

This work investigated the electrochemical behavior of $Ti_3C_2T_x$ electrodes in various concentrations of methanesulfonic acid, an environmentally friendly electrolyte. The behavior in 4 M MSA was particularly attractive, competing with $Ti_3C_2T_x$ in H_2SO_4. For example, capacitance of 294 F g^{-1} at 10 A g^{-1} was obtained with excellent cycle life. The cyclic voltammograms exhibits a couple of symmetric redox peaks, which suggest a pseudocapacitive behavior.[30] Interestingly, a concept of hydronium-ion battery was previously proposed, using perylenetetracarboxylic dianhydride as an electrode in H_2SO_4,[31] and $Ti_3C_2T_x$ in 4 M MSA could be an alternative system.

The charge storage mechanism was investigated by in-situ XRD, ex-situ XPS, and compared with H_2SO_4 and CH_3SO_3Na electrolytes. Results demonstrated a faradaic mechanism attributed to intercalation/de-intercalation of H$^+$ or H$_3$O$^+$ between $Ti_3C_2T_x$ layers, which may be accompanied by co-intercalation of $CH_3SO_3^-$. The co-intercalation hypothesis proposed here still requires direct evidence and independent confirmation by other techniques capable of detecting confined ions, such as nuclear magnetic resonance. Modeling and simulation would help to fully understand the intercalation process and possibility of co-intercalation of anions into $Ti_3C_2T_x$ and other MXenes. Additionally, owing to the large expansion and shrinkage of the c-lattice parameter over a small potential window, $Ti_3C_2T_x$ in 4 M MSA is promising for designing high performance electrochemical actuators.

Considering that this is the first report on electrochemical behavior of MXene in MSA, we selected the conventional $Ti_3C_2T_x$ MXene electrode with restacked nanosheets, but it is not assumed to be the optimal MXene-based electrode. It was reported that V_2CT_x,[14] $Ti_3C_2T_x$ hydrogel, 3D macroporous $Ti_3C_2T_x$,[16] $Ti_3C_2T_x$ composites, and $Ti_3C_2T_x$ with vertically-aligned nanosheets[23] electrodes exhibited higher performances than in-plane aligned $Ti_3C_2T_x$ film in H_2SO_4. Thus, it can be expected that other MXene compositions and morphologies can further improve the electrochemical performance in MSA.

Experimental Section

Materials: methanesulfonic acid (MSA CH$_3$SO$_3$H), sodium methanesulfonate (CH$_3$SO$_3$Na) and sulfuric acid (H$_2$SO$_4$) were purchased from Aladdin and used as received or diluted in distilled water. $Ti_3C_2T_x$ was synthesized by selective etching of Ti_3AlC_2 in LiF and HCl mixture as previously described elsewhere.[32] Briefly, 1 g of Ti_3AlC_2 powder (400 mesh, purchased from Jilin 11technology Co.) was slowly added to an etchant solution containing 0.8 g LiF and 10 mL of 9 M HCl, then stirred for 24 hours at 35°C. The acidic mixture was washed with distilled water via centrifugation for 5 min per cycle at 8000 rpm until pH ≈ 6. Wet $Ti_3C_2T_x$ paste was casted between Celgard membranes using a glass tub into film and dried at room temperature. Then, $Ti_3C_2T_x$ film was cut into 3-mm radius circle electrodes.

Electrochemical testing : The electrochemical behavior was investigated using a VMP3 potentiostat (Biologic, S.A.) with three-electrode Swagelok cells, where 9 μm thick $Ti_3C_2T_x$ with mass loadings of 1.77 mg cm^{-2} was the working electrode, overcapacitive $Ti_3C_2T_x$ was the counter electrode, polypropylene membrane was the separator, and Ag wire was used as reference electrode. Electrochemical impedance spectroscopy (EIS) measurements were performed from 0.01 Hz to 100 kHz at open circuit voltage (OCV). The capacitance was calculated by integration of current with respect to time, according to the following equation:

$$C = (\int_0^{\frac{V}{s}} idt)/(sVm)$$

Where C is the gravimetric capacitance (F g^{-1}), i is the gravimetric current density (A), s is the scan rate (V s^{-1}), and V is the potential window (V).

Materials characterization: *In-situ* X-ray diffraction (XRD) patterns were collected using a Bruker D8 diffractometer operated at 40 kV and 40 mA using a Cu Kα radiation (λ = 1.5406 Å) in the range 2θ=5–20° with a step of 0.01°. The sample was placed in a 3-electrode cell and covered with a Kapton window to avoid electrolyte evaporation, allowing *in-situ* XRD recording. The XRD patterns were recorded each 0.008 mV while cyclic voltammetry at 0.2 mV s^{-1} was used in order to control the cell potential. The data presented were obtained after a few cycles.

X-ray photoelectron spectrometry (XPS, ESCALAB) was carried out for analyzing the composition of electrodes and the oxidation state of elements using a Mg-K$_\alpha$ light source. XPS measurements were performed on pristine Ti$_3$C$_2$T$_x$ and polarized electrodes, which were held for 2 hours at -0.9 V and 0.1 V *vs*. Ag in 4 M MSA after 10 cyclic voltammetry (CV) cycles at 2 mVs^{-1}. Then, samples were washed with DI water to avoid influence of electrolyte residue.

[1] a) B. Anasori, M. R. Lukatskaya, Y. Gogotsi, *Nature Reviews Materials* **2017**, *2*, 16098; b) M. Naguib, M. Kurtoglu, V. Presser, J. Lu, J. Niu, M. Heon, L. Hultman, Y. Gogotsi, M. W. Barsoum, *Advanced Materials* **2011**, *23*, 4248-4253.

[2] M. Naguib, V. N. Mochalin, M. W. Barsoum, Y. Gogotsi, *Advanced Materials* **2014**, *26*, 992-1005.

[3] a) S. Xu, Y. Dall'Agnese, J. Li, Y. Gogotsi, W. Han, *Chemistry – A European Journal* **2018**, *24*, 18556-18563; b) J. Pang, R. G. Mendes, A. Bachmatiuk, L. Zhao, H. Q. Ta, T. Gemming, H. Liu, Z. Liu, M. H. Rummeli, *Chemical Society Reviews* **2019**, *48*, 72-133.

[4] A. Sinha, Dhanjai, H. Zhao, Y. Huang, X. Lu, J. Chen, R. Jain, *TrAC Trends in Analytical Chemistry* **2018**, *105*, 424-435.

[5] M. Han, X. Yin, K. Hantanasirisakul, X. Li, A. Iqbal, C. B. Hatter, B. Anasori, C. M. Koo, T. Torita, Y. Soda, L. Zhang, L. Cheng, Y. Gogotsi, *Advanced Optical Materials* **2019**, *7*, 1900267.

[6] Q. Hu, D. Sun, Q. Wu, H. Wang, L. Wang, B. Liu, A. Zhou, J. He, *Journal of Physical Chemistry A* **2013**, *117*, 14253.

[7] F. Shahzad, M. Alhabeb, C. B. Hatter, B. Anasori, S. Man Hong, C. M. Koo, Y. Gogotsi, *Science* **2016**, *353*, 1137-1140.

[8] a) C. Dall'Agnese, Y. Dall'Agnese, B. Anasori, W. Sugimoto, S. Mori, *New Journal of Chemistry* **2018**, *42*, 16446-16450; b) L. Yang, Y. Dall'Agnese, K. Hantanasirisakul, C. E. Shuck, K. Maleski, M. Alhabeb, G. Chen, Y. Gao, Y. Sanehira, A. K. Jena, L. Shen, C. Dall'Agnese, X.-F. Wang, Y. Gogotsi, T. Miyasaka, *Journal of Materials Chemistry A* **2019**, *7*, 5635-5642.

[9] K. Huang, Z. Li, J. Lin, G. Han, P. Huang, *Chemical Society Reviews* **2018**, *47*, 5109-5124.

[10] M. R. Lukatskaya, O. Mashtalir, C. E. Ren, Y. Dall'Agnese, P. Rozier, P. L. Taberna, M. Naguib, P. Simon, M. W. Barsoum, Y. Gogotsi, *Science* **2013**, *341*, 1502-1505.

[11] R. B. Rakhi, B. Ahmed, M. N. Hedhili, D. H. Anjum, H. N. Alshareef, *Chemistry of Materials* **2015**, *27*, 5314-5323.

[12] J. Halim, S. Kota, M. R. Lukatskaya, M. Naguib, M.-Q. Zhao, E. J. Moon, J. Pitock, J. Nanda, S. J. May, Y. Gogotsi, M. W. Barsoum, *Advanced Functional Materials* **2016**, *26*, 3118-3127.

[13] Q. Tao, M. Dahlqvist, J. Lu, S. Kota, R. Meshkian, J. Halim, J. Palisaitis, L. Hultman, M. W. Barsoum, P. O. Å. Persson, J. Rosen, *Nature Communications* **2017**, *8*, 14949.

[14] Q. Shan, X. Mu, M. Alhabeb, C. E. Shuck, D. Pang, X. Zhao, X.-F. Chu, Y. Wei, F. Du, G. Chen, Y. Gogotsi, Y. Gao, Y. Dall'Agnese, *Electrochemistry Communications* **2018**, *96*, 103-107.

[15] a) J. Yan, C. E. Ren, K. Maleski, C. B. Hatter, B. Anasori, P. Urbankowski, A. Sarycheva, Y. Gogotsi, *Advanced Functional Materials* **2017**, *27*, 1701264; b) Y. Dall'Agnese, P. Rozier, P.-L. Taberna, Y. Gogotsi, P. Simon, *Journal of Power Sources* **2016**, *306*, 510-515; c) N. C. Osti, A. Gallegos, B. Dyatkin, J. Wu, Y. Gogotsi, E. Mamontov, *The Journal of Physical Chemistry C* **2018**, *122*, 10476-10481.

[16] M. R. Lukatskaya, S. Kota, Z. F. Lin, M. Q. Zhao, N. Shpigel, M. D. Levi, J. Halim, P. L. Taberna, M. Barsoum, P. Simon, Y. Gogotsi, *Nature Energy* **2017**, *2*, 6.

[17] M. Hu, Z. Li, T. Hu, S. Zhu, C. Zhang, X. Wang, *ACS Nano* **2016**, *10*, 11344-11350.

[18] M. D. Gernon, W. Min, T. Buszta, P. Janney, *Green Chemistry* **1999**, *1*, 127-140.

[19] a) D. Pletcher, H. Zhou, G. Kear, C. T. J. Low, F. C. Walsh, R. G. A. Wills, *Physical Chemistry Chemical Physics* **2004**, *6*, 1779-1785; b) F. C. Walsh, C. P. D. León, *Surface & Coatings Technology* **2014**, *259*, 676-697.

[20] M. Krishna, E. J. Fraser, R. G. A. Wills, F. C. Walsh, *Journal of Energy Storage* **2018**, *15*, 69-90.

[21] C. Zhan, M. Naguib, M. Lukatskaya, P. R. C. Kent, Y. Gogotsi, D.-e. Jiang, *The Journal of Physical Chemistry Letters* **2018**, *9*, 1223-1228.

[22] X. Wang, T. S. Mathis, K. Li, Z. Lin, L. Vlcek, T. Torita, N. C. Osti, C. Hatter, P. Urbankowski, A. Sarycheva, M. Tyagi, E. Mamontov, P. Simon, Y. Gogotsi, *Nature Energy* **2019**, *4*, 241-248.

[23] Y. Xia, T. S. Mathis, M.-Q. Zhao, B. Anasori, A. Dang, Z. Zhou, H. Cho, Y. Gogotsi, S. Yang, *Nature* **2018**, *557*, 409-412.

[24] M.-Q. Zhao, N. Trainor, C. E. Ren, M. Torelli, B. Anasori, Y. Gogotsi, *Advanced Materials Technologies* **2019**, *4*, 1800639.

[25] a) X. Mu, D. Wang, F. Du, G. Chen, C. Wang, Y. Wei, Y. Gogotsi, Y. Gao, Y. Dall'Agnese, *Advanced Functional Materials* **2019**, *0*, 1902953; b) M. Ghidiu, J. Halim, S. Kota, D. Bish, Y. Gogotsi, M. W. Barsoum, *Chemistry of Materials* **2016**, *28*, 3507-3514.

[26] O. Mashtalir, M. Naguib, V. N. Mochalin, Y. Dall'Agnese, M. Heon, M. W. Barsoum, Y. Gogotsi, *Nature Communications* **2013**, *4*, 1716.

[27] A. C. Forse, J. M. Griffin, C. Merlet, P. M. Bayley, H. Wang, P. Simon, C. P. Grey, *Journal of the American Chemical Society* **2015**, *137*, 7231-7242.

[28] a) A. P. Kirilova, V. D. Maiorov, A. I. Serebryanskaya, N. B. Librovich, E. N. Gur'yanova, *Bulletin of the Academy of Sciences of the USSR, Division of chemical science* **1987**, *36*, 2525-2529; b) A. P. Kirilova, V. D. Maiorov, A. I. Serebryanskaya, N. B. Librovich, E. N. Gur'Yanova, *Bulletin of the Academy of Sciences of the USSR Division of Chemical Science* **1985**, *34*, 1366-1371.

[29] C. Shen, L. Wang, A. Zhou, B. Wang, X. Wang, W. Lian, Q. Hu, G. Qin, X. Liu, *Nanomaterials* **2018**.

[30] H. Shao, Z. Lin, K. Xu, P.-L. Taberna, P. Simon, *Energy Storage Materials* **2019**, *18*, 456-461.

[31] X. Wang, C. Bommier, Z. Jian, Z. Li, R. S. Chandrabose, I. A. Rodríguez-Pérez, P. A. Greaney, X. Ji, *Angewandte Chemie International Edition* **2017**, *56*, 2909-2913.

[32] M. Alhabeb, K. Maleski, B. Anasori, P. Lelyukh, L. Clark, S. Sin, Y. Gogotsi, *Chemistry of Materials* **2017**, *29*, 7633-7644.

Entry for the Table of Contents (Please choose one layout)

Layout 1:

FULL PAPER

Two-dimensional titanium carbide ($Ti_3C_2T_x$ MXene) has gained much attention as electrode for supercapacitors with a common sulfuric acid electrolyte. In this work, attractive performance is achieved with a more environmentally friendly alternative acidic electrolyte, methanesulfonic acid. The largest reversible volume change in MXenes in aqueous electrolytes is observed.
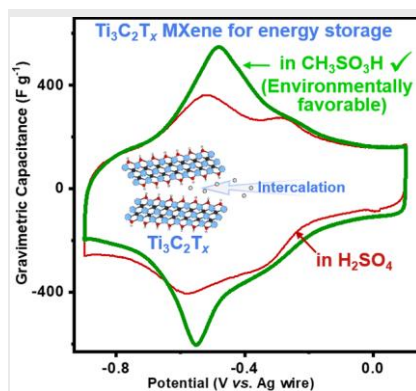
Xin Zhao, Chunxiang Dall'Agnese, Xue-Feng Chu, Shuangshuang Zhao, Gang Chen, Yury Gogotsi, Yu Gao*, Yohan Dall'Agnese*

Page No. – Page No.

Electrochemical Behavior of $Ti_3C_2T_x$ MXene in Environmentally Friendly Methanesulfonic Acid Electrolyte